Iraqi Journal of Veterinary Sciences

www.vetmedmosul.com

Study the role of KSper current for controlling the Ca2+ influx and intracellular pHi in mouse spermatozoa by dominating membrane potentials

S.M.A. Alghazal[1] and J. Ding[2]

[1] Department of Physiology, Biochemistry and Pharmacology, College of Veterinary Medicine, University of Mosul, Mosul, Iraq, [2] Key Laboratory of Molecular Biophysics of Ministry of Education, College of Life Science and Technology, Huazhong University of Science and Technology, Wuhan 430074, China

Article information

Article history:
Received March 19, 2019
Accepted August 31, 2019
Available online June 17, 2022

Keywords:
Fertility
Ca^{2+} channel
Ko mice
Cation channel

Correspondence:
S.M.A. Alghazal
suhamd2001@yahoo.com

Abstract

This work was aimed to explore the details of the ion channels gating and there physiological role in sperm in the future. Mouse spermatozoa express a pH-dependent K^+ current (KSper) thought to induce hyperpolarization to enhance Ca^{2+} influx via alkaline-activated calcium channel (Catsper) to initial a so-called sperm capacitation by NH_4Cl during travelling in female genital tract for fertilization. However, the regulating mechanism of the Ksper and Catsper channels by membrane potential and pH_i remains uncertain, because the complexities of two channel kinetics in sperms is hardly to be overcame at this stage. Here we show that difference of the intracellular $[Ca^{2+}]_i$ between the wild type (Wt) and knockout (KO) Ksper (or $Slo3^{-/-}$) mice in the application of the Slo3 blockers, Guinidine (QD) and Clofilium, and NH_4Cl, indicating that Ksper channels, encoding Slo3 gene, dominates the membrane potential of mouse sperms to increase the intracellular $[Ca^{2+}]_i$ and $[pH]_i$ during the capacitation process to play a vital role in fertility. Furthermore, a HH model sperm built directly with the native Ksper and Catsper currents in sperms reveals two functions of membrane potential and intracellular pH_i, allowing us to calculate the intracellular pH_i by NH_4Cl, based on membrane potentials recording from current-clamp experiments. During modeling, we found a caton channel with V_{rev}= +20 mV in mouse sperm from the double-KO (i.e. $Catsper^{-/-}$ and $Ksper^{-/-}$) mice, which is definitely necessary for a model able to match the data.

DOI: 10.33899/ijvs.2019.125493.1023,

Introduction

An alkalization-activated K^+ channel (KSper) in mouse sperm, encoding by the Slo3 gene (1-3) is responsible for the capacitation of sperms as they travel through the female genital tract (4-6).These changes includes an increase in the intracellular pH (pH_i) (7), sperm membrane hyperpolarization (8) and intracellular Ca^{2+} elevation (9), although an increases in $[Ca^{2+}]_i$ and intracellular $[pH]_i$ are approved to play a vital roles in both sperm capacitation and the acrosome reaction (AR) (6,10). Except for Ksper channel, there is another major alkalization-activated ion channel, Catsper Ca^{2+} channel in mouse sperm. It has been shown that the genetic knockout (KO) of either of these channel genes confers male infertility indicating that both of these channels play a vital role in sperm physiology (2,11) .During capacitation, both become active by NH_4Cl , which is thought to act via cytosolic alkalization. Several types of these transporters such as the Na^+/ H^+ exchanger, a Na^+- Cl^-/

$HCO3^-$ transporter, and a $Na^+/HCO3^-$ transporter have been proposed to participate in sperm alkalization during capacitation (12). Upon membrane hyperpolarization ,this transport mechanism launches to increase intracellular Ca^{2+} following the rapidly rising surge of pHi in mouse sperm. However , it remains unclear how membrane potentials regulate the intracellular pHi and Ca^{2+} influx in mouse sperm (13). The inhibition of Ksper channel by the Slo3 channel blockers Quinidine (QD) and Clofilium (13) decreases the intracellular [Ca2+]i , specially establish a sperm model cell to illustrate the capacitation mechanism and confer two functions of membrane potential and intracellular pHi during alkalization.Furthermore ,we revealed a cation channel in sperm from the double-KO (i.e. Catsper -/- and Ksper -/-) mice, which is definitely necessary for the model able to match the data. The model we proposed here may allow us to quantitatively calculate the membrane potential Vm, the intracellular pHi and $[Ca^{2+}]i$ under various different condtions for better understanding of the mechanisms occurring in mouse sperms.

Materials and Methods

Reagents

All reagents and chemicals were purchased from Sigma-Aldrich Co. (St. Louis, MO) with the following exceptions unless otherwise stated.Fluo4-AM and pluronic F-127 were obtained from Molecular Probes (Invitrogen, Eugene,OR).Cell-Tak wasfrom BD Biosciences (Bedford, MA). Quinidine ,Clofilium ,NH_4Cl were from sigma Co. Supplemented Hank solution (HS) contained in mM: 135 NaCl , 5 KCl , 2 $CaCl_2$, 1$MgCl_2$, 30 HEPES , 10 Glucose, 10 Lactic Acid , 1 Napyrovate, adjusted to PH 7.4 with NaOH (14).

Animals and Cell Preparation

Wild type (WT) mice were used in the study, followed the guidelines approved by AAALAC Intl (center for Animal Care) of Wuhan University,while Slo3 knock-out mice were obtained from Chris Lingle's lab, Washington University in St. Louis, St.Louis, MO, USA.An adult male mice were used in experiments for sperm collection, 3- to 6-month olds. Mice were killed with CO_2 asphyxiation, followed by cervical dislocation. Caudal epididymids were excised and rinsed with HS medium.Sperms were released from three small incisions at 37.8C° and 5 % CO_2 incubator for 15 min into HS medium supplement. Released sperm were concentrated to 5×10^6 to 10^7 /ml by centrifugation at 500 g for 5 minutes (15).

Ca^{2+} imaging

Cells were loaded with 4 µM Fluo-4 AM and 0.05 % Pluronic F-127 for 30 min. at room temperature in the dark, followed by two washes with the imaging medium (HS). Washed sperm were plated onto coverslips coated with Cell-Tak. Small-volume imaging chambers (~1 cm diameter [90 µl]) were formed with Sylgard on coverslips. Cells were allowed to attach for 10 min (16). Andor Technology (springvale Business park, Belfast ,UK) with a 75-W xenon lamp was used to generate the excitation at 491 nm. A 60× objective and a 1.63 adaptor on an inverted microscope (IX-71; Olympus,UK) were used for imaging.Emissions (491 nm) were band pass filtered (HQ540/50; Chroma, Rockingham, VT) and collected with a cooled charge-coupled device camera (CoolSNAP HQ; Roper Scientific, Tucson, AZ) for 300 repeat interval at every 5 sec. Online control, data collection, and image processing were done using commercial software imaging analysis were performed on the whole sperm, using a software image J. $[Ca^{2+}]_i$ changes are presented as $F:F_0$ ratios after background subtraction , where F is the fluorescence signal intensity and F_0 is the baseline as calculated by averaging the 10-20 frames before stimulus application. Cells with uneven dye loading were excluded from analysis, even motile sperm, Raw intensity values were imported into sigma plot analyzing program and normalized utilizing the equation: $(F/F_0)\times100$ % , F = is fluorescence intensity, F_0 is the fluorescence intensity before stimuli, which is a mean of 10-20 determinations of F obtained during the control period.The final normalized fluorescence intensity is represented as F/F_0 (%). Quinidine (0.1, 1, 10, 100, 1000 µM) and Clofilium (50, 100, 500 µM) were added to the imaging chamber by multiple plastic tubes connecting to a perfusion pipette (16).

Statistical Analysis

Data analysis were performed using Image-J software, Raw intensity values were imported into sigma plot analyzing software, Data represented as mean ± S.E.
The dose-response curve was plotted by using standard curve analysis based on a four-parameter logistic in Sigma Plot software according to the following equation:
Inhibition of fluorescence intensity (%) $=1/(1+IC_{50}/[T])$ (1).

Mathematical modeling and simulation

Our spermium cell model can be described as the following equation (17):

$$C*dV/dt= I_{CatSper} +I_{KSper}+I_{cation}+I_{task} \quad (2)$$

where V is the membrane potential in mV, C is the capacity of the cell membrane in pF, t is the time in ms, the $I_{CatSper}$ is the CatSper current in pA, the I_{KSper} is the KSper current in pA, the I_{cation} is the cation current in pA, and the I_{task} is the task current in pA.

CatSper current:

$I_{CatSper}=G*(V-V_r) =ng*P_o*(V-V_r)$ (3).

$$Po = \frac{(I_0+a\times V)}{(V-V_O)\times n_0\times g}\times k[H^+] \quad (4).$$

$$k[H^+] = y_0 + b * \exp(-c * [H^+]) \quad (5).$$

Where coefficients I_0=-3.5837, a=0.0761, b=1.0474, c=5.77, y_0=0.02, reversal potential in the experiment cell V_o= 47.1 mV, reversal potential in the model V_r=70 (mV) (18) and k is the pH-dependent factor (19) of $I_{CatSper}$ currents (Figure 1B). And , g is the single-channel conductance, n_0 is the number of channels in an experimental cell and n is the number of channels in the model cell and n/n_0= 0.7543.

Thus, we have

$$I_{CatSper} = 0.7543 \times \frac{(-3.5837+0.0761\times V)}{(V-47.1)} \times (0.02 + 1.0474 * \exp(-5.77 * [H^+])) \times (V - 70) \quad (6).$$

KSper currents:

$I_{KSper}=G*(V-V_r) =ng*P_o*(V-V_r)$ (7).

$$Po = I_{-\infty} \times \frac{1-exp(a1\times(V-V_{off})}{n_0\times g\times(V-V_{off})} \times k1[H^+] \quad (8).$$

$k[H^+]= b1*\exp(c1/([H^+]+d1))$ (9).

$I_{KSper}= (n/n_0)* I_{-\infty}*(1-\exp(a1*(V-V_{off})))/(V-V_{off})*(V-V_r) * k[H^+]$ (10).

Where $I_{-\infty}$=-223.7001, a1=0.0134 (1/mV), b1=0.0395, c1=1.2221 (µM), d1=0.3684 (µM), the offset of I_{kSper} in the experiment cell V_{off} = -5.6626 mV, reversal potential in the model V_r = -70 (mV) (20) , g is the single-channel conductance, n_0 is the number of channels in the experimental cell and n is the number of KSper channels in the model cell and n/n_0=0.2898.

Thus, we have

$$I_{KSper} = 0.2898 \times (-223.7001) \times \frac{1-\exp(0.0134\times(V+5.6626)}{(V+5.6626)} \times 0.0395 \times exp(1.2221/([H+] + 0.3684)) \times (V + 65) \quad (11).$$

Cation current:

$I_{Cation}=G*(V-V_r) =ng*P_o*(V-V_r)$ (12)

$$Po = \frac{(I_1+e\times V)}{(V-V_1)\times n_0\times g} \times k[pH] \quad (13)$$

$k[pH]=0.0628+0.1172*pH$ (14)

Where coefficients I_1= -2.7525, e=0.0863, reversal potential in the experiment cell V_1=32 mV, reversal potential in the model V_r=16 (mV) . and k is the pH-dependent factor of I_{Cation} currents (Figure 1C). And, g is the single-channel conductance, n_0 is the number of channels in the experimental cell, and n is the number of channels in the model cell and n/n_0= 3.5.

Thus, we have

$$I_{Cation} = 3.5 \times \frac{(-2.7525+0.0863\times V)}{(V-32)} \times (0.0628 + 0.1172 \times pH) \times (V - 16) \quad (15).$$

Task current:

$I_{task}=G*(V-V_r) =G_{max}*P_o*(V-V_r)$

Where G_{max}=0.105 nS, P_o=1 and V_r=-85 mV (21).

The converting expression of Ca^{2+} and $I_{CatSper}$ can be expressed as below,

$$\frac{d[\mathrm{Ca}]_i}{dt} = e_{trans} \times I_{CatSper} - e_{diff} \times [\mathrm{Ca}]_i \quad (16).$$

Where the e_{trans} is the converting coefficient of $I_{CatSper}$ and $[Ca^{2+}]_i$ and the e_{diff} is the diffusing coefficient of $[Ca^{2+}]_i$

Results

Effects of Quinidine (QD) and Clofilium on the Ca^{2+} influx into wild type (WT) mouse sperms

Using the indicator Fluo-4 AM with a highly sensitivity to Ca^{2+}, The results showed the spatial-temporal heterogeneous changes in $[Ca^{2+}]_i$ in the cellular sub-domains along the sperm. Comparing with its head and middle regions, the tail region always showed the weakest fluorescence intensity before applying the QD or Clofilium (Figure 1C and Figure 2C). Therefore, only the head region was used for measuring the changes of fluorescence intensity in this study. In the Figure 1A, the chemical QD, a typical inhibitor of K^+ channel induced a completely reversible reduction in the intracellular Ca^{2+} of sperms at the lower concentration (0.1 and 1 µM), but a partially reversible reduction at the higher concentrations (10, 100 and 1000 µM)., Furthermore, a dose-response curve of QD reducing Ca^{2+} influx showed an IC_{50} = 44.2 ± 2.1 µM (n ≥ 3) (Figure 1B). Clofilium has been demonstrated to irreversibly block KSper. The corresponding changes in Ca^{2+} influx into wt sperm caused by Clofilium were also manifested with a decreasing F / F_0 (%) after exposure to Clofilium for ~300 sec. (Figure 2A). With the application of 500, 100 and 50 µM Clofilium to sperms loaded with Flu4-AM, the relative fluorescence intensities were respectively 56 ± 3.34 % (n = 6) for 500 µM Clofilium, 48 ±1.8 (n= 4) for 100 µM Clofilium and 38 ± 5.9 (n= 3) for 50 µM Clofilium (Figure 2B). Before applying the inhibitors such as QD and Clofilium , there were stronger fluorescence intensities in wt sperms. With the application of QD, the fluorescence intensities in wt sperms were becoming much weaker, and then got a part of recovery in intensity during washout with HS for a few minutes (Figure 1C). In contrast, with the application of Clofilium, the fluorescence intensities in Wt sperms were becoming much weaker too, but then got no recovery at all during washout with HS for a few minutes (Figure 2C).

NH_4Cl enhances $[Ca^{2+}]_i$ in sperm

The results showed an elevation in the intracellular Ca^{2+} in wt sperms treated with 10 mM NH_4Cl (Figure 3A and 3C). Moreover, the application of 10 µM QD +10 mM NH_4Cl reduced the Ca^{2+} in wt sperm with a reversible recovery after washout by 10 mM NH_4Cl (Figure 3B). In contrast, the application of 50 µM Clofilium +10 mM NH_4Cl caused inhibition of Ca^{2+} entering into wt sperm with a slightly reversible recovery after washout by 10 mM NH_4Cl (Figure 3D). Therefore, NH_4Cl triggered a $[Ca^{2+}]_i$ elevation in wt

sperm under the inhibition conditions caused either by QD or by Clofilium.

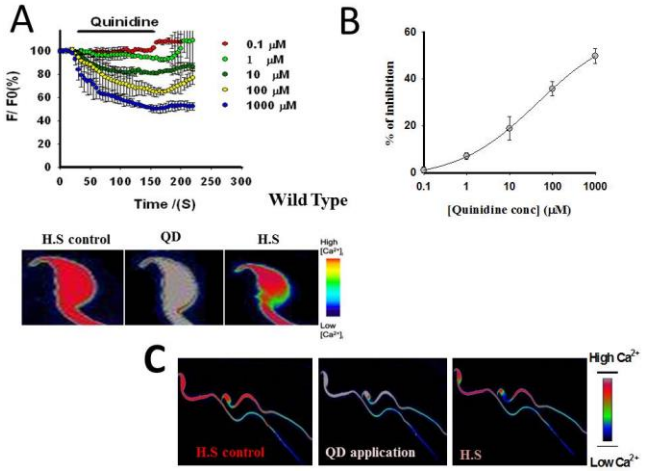

Figure 1: An inhibitor of Catsper and Ksper channels, quinidine (QD) reduces the Ca^{2+} influx into the mouse sperms. (A) The relative fluorescence intensities (F/F_0) (%) in $[Ca^{2+}]_i$, in the presence of 0.1,1,10,100 and 1000 μM QD, were plotted as the function of the elapsed time. Here the F denotes the measured fluorescence intensities and F_0 the mean basal fluorescence intensity, in the presence and absence of QD, respectively. The black horizontal bar represents the application of QD. A typical example, as indicated, from a single sperm was placed at the bottom. A scale bar was placed at the right. (B) A dose–response curve was plotted for QD blocking Ca^{2+} signal shown in (A). A solid line was a fit to Eq. 1. Here IC_{50} = 44.2 ± 2.1 μM (n≥3). (C) Three representative Ca^{2+} images were took from two sperms bathed in Hank solution loaded with the flu4-Am and pluronic F-127 at 37ºC, in the presence and absence of QD as indicated, respectively, under a 75-w Xenon lamp, generating an exciting light of 491 nm, with a 60x objective and a 1.6 adaptor on an inverted microscope. A scale bar was placed at the right. Data collection and imaging analysis were performed on the whole sperm , using a software ImageJ (See the methods and Materials).

The characteristics of Ca^{2+} influx into the Slo3-KO mouse sperms

In this study, the Slo3-KO mouse was used to further demonstrate that all of the above phenomena are derived from KSper (or Slo3) channels. As a comparison, we re-examined the changes of Ca^{2+} signal in the Slo3-null mouse sperms under similar conditions as described previously (Figure 1-3). The fluorescence intensities of Ca^{2+} in $Slo3^{-/-}$ sperms (Figure 4A and 4B) were reduced significantly by applying either 10 μM QD or 50 μM Clofilium, which are the same to that in Wt sperms (Figure 1 and 2). Compared with the Wt sperms, the $Slo3^{-/-}$ sperms showed a complete recovery in Ca^{2+} signal from the Clofilium inhibition due to no irreversible factor Slo3. Additionally, the application of 10 mM NH_4Cl also enhanced the Ca^{2+} signal in $Slo3^{-/-}$ sperms (Figure 4C and 4D), similar to that we described previously in Wt sperms (Figure 3).

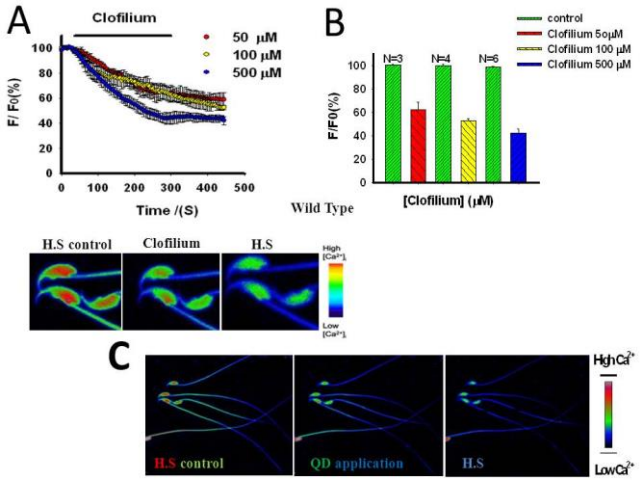

Figure 2: An inhibitor of Catsper and Ksper channels, clofilium decreases the Ca^{2+} influx into the mouse sperms. (A) Clofilium inhibited the $[Ca^{2+}]_i$ entry into sperm, bathed in H.S. pH7.4 containing 2 mM Ca^{2+}, of which the relative fluorescence intensities (F/F_0) in $[Ca^{2+}]_i$(%), in the presence of 50,100 and 500 μM Clofilium, were plotted as the function of the elapsed time. The black horizontal bar represents the application of Clofilium. A typical example, as indicated, from three sperms was placed at the bottom. A scale bar was placed at the right. (B) A statistics of the relative Clofilium inhibition on Ca^{2+} entry to sperm after exposure to Clofilium for about 300 seconds. The relative Clofilium inhibitions were respectively 56.0±3.3 % for 500 μM (n= 6) , 48.0±1.8 % for 100 μM (n= 4) and 38.0± 5.9 % for 50 μM (n = 3) as indicated. (C) Three representative Ca^{2+} images were took from five mouse sperms bathed in Hank solution (pH7.4) loaded with the Fluo-4Am, in the presence and absence of Clofilium as indicated. A scale bar placed at the right.

Slo3 dominates the membrane potentials in sperms

Base on the current-clamp experiments of sperms, the membrane potentials were measured under two intracellular $[pH]_i$ as shown in Figure 5. The sperms containing Slo3 in Figure 5 showed the more negative membrane (resting) potentials at the higher pH. However, the resting potentials of Slo3-KO sperms were opposite.

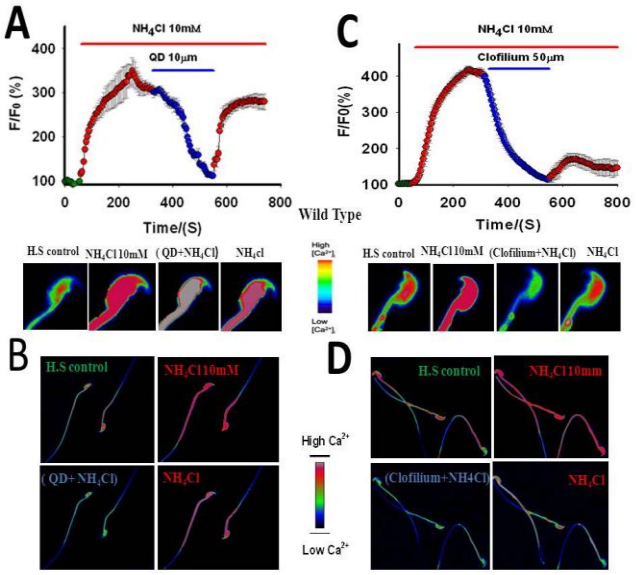

Figure 3: Alkalization of NH_4Cl increases the intracellular $[Ca^{2+}]_i$ in mouse sperms. (A) The relative fluorescence intensities (F/F_0) (%) in $[Ca^{2+}]_i$, in the presence of control (Green),10 mM NH_4Cl (Red) and 10 μM QD+10 mM NH_4Cl (n = 4) (Blue) as indicated, were plotted as the function of the elapsed time. A typical example from a single sperm as indicated was placed at the bottom. A scale bar was placed at the right. (B) Four representative Ca^{2+} images were took from two mouse sperms bathed in Hank solution (pH 7.4) loaded with the flu4-Am, in the presence and absence of Clofilium as indicated. A scale bar placed at the right. (C-D) All the same except for 50 μM Clofilium (n = 4) as we described in (A) and (B).

Simulation for the membrane potential of sperms

To simulate the membrane potentials of sperms, we need to construct a model cell composed of the several major model channels in sperms, of which currents should satisfy an ordinary differential equation (Eq. 2). Typically, the only unknown open probability P_o of model channels can be accurately calculated from the kinetic model of model channels and then the currents of model channels can be obtained from $I=NgP_o(V-V_r)$ (Eq. (3)). However, it is too difficult to have their respective kinetic models for the CatSper and KSper channels in the sperm's case. As a substitute, an alternative method is to approximatively fit the voltage-ramp current to a mathematic expression (or a formula), which can be used to get the Po of a model channel. In other words, a dynamic kinetic model is replaced by a quasi-steady-state formulation model. Obviously, it is at the expense of the loss of accuracy. As a qualitative analysis, however, it may be worth to do so. Considering that the entire channels including CatSper and KSper in sperms show the quasi-linear currents during a ramp voltage, we thus fit these currents to their respective mathematic expressions in order to build their model channels.

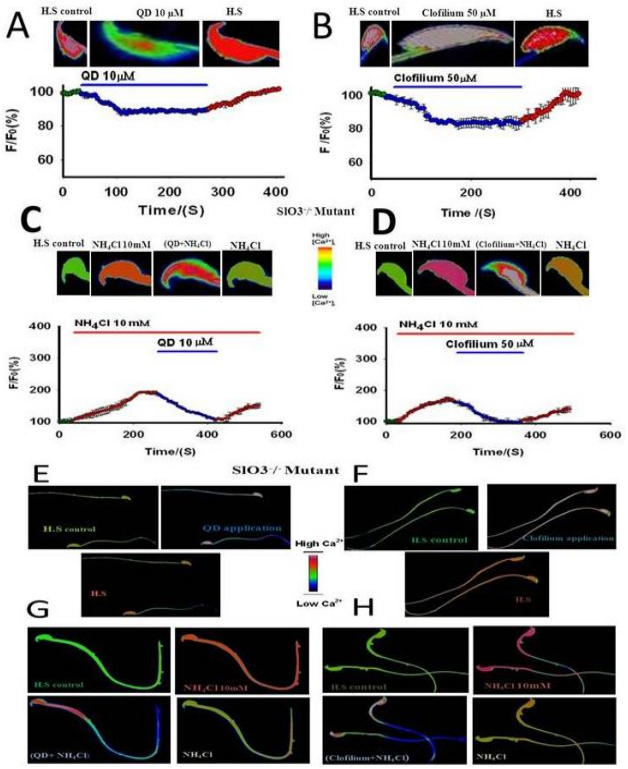

Figure 4: The effects of QD, Clofilium and NH_4Cl on the $Slo3^{-/-}$ sperms. (A-B) Cells from two Slo3-null mice were imaged with Flu4 -AM, of which F/F_0 showed an initial 11 % decrease caused either by 10 μM QD (n = 4) and 17% by 50 μM Clofilium (n = 4), and then a complete recovery after H.S washout at pH7.4. (C-D) 10 mM NH_4Cl induced an initial increase in the relative fluorescence intensities and then an inhibition either by applying 50 μM Clofilium+10 mM NH_4Cl (n = 5) or by 10 μM QD +10 mM NH_4Cl (n = 5), following by a partially reversible recovery in both cases after 10 mM NH_4Cl washout. (E-H) The representative images showed the $[Ca^{2+}]_i$ changes evoked by the above stimuli along the flagella of $Slo_3^{-/-}$ sperms. The changes of the Ca^{2+} signals started from the tail, and then propagated to the head.

In this study, the model sperm cell was composed of the CatSper, KSper, Cation and leak channels (See the Methods and Materials). Then, those models can be used to calculate their currents occurring in the model sperm cell as well as the membrane potential of model cell (Figure 6A and 6B).To determine the mathematic expression for each of model channels, an exponential or a linear function was firstly chosen to match the ramp currents recorded at pH=8.0. Secondly, a $k(H^+)$ factor of the above expression was also

needed to be determined based on the currents at different pH normalized to that of pH=8.0. To more easily select the appropriate expression for a ramp trace, we introduced a V_{off} to shifted the origin of V-axis to the zero-current voltage. For example, we chose a linear function with a V_{off} = 47.1 mV to match the ramp currents of CatSper recorded at pH=8.0 (Eq. 4), of which the factor k(H^+) came from the currents recorded at a variety of pH (Figure 6A). Notably, we ignored the rapid decline in part on the starting ramp current of CatSper, as the CatSper channel was not in a stable state at the beginning of ramp (Figure 6A left). Alternatively, the larger amount of Na^+ not Ca^{2+} entered probably into channel at the starting time of ramp. Similarly, we built the KSper model channel with an exponential function with V_{off} = -5.7 mV under symmetrical K^+ solutions (Figure 6B). Based on the model sperm cell composed of the CatSper, KSper, cation and leak (or task) channels, we simulated respectively the membrane potentials at different pH in wt and $Slo3^{-/-}$sperms and further constitute two functions for them to describe the relationship between the V_m and pH (Figure 6C), consistent to the results shown in Figure 5.

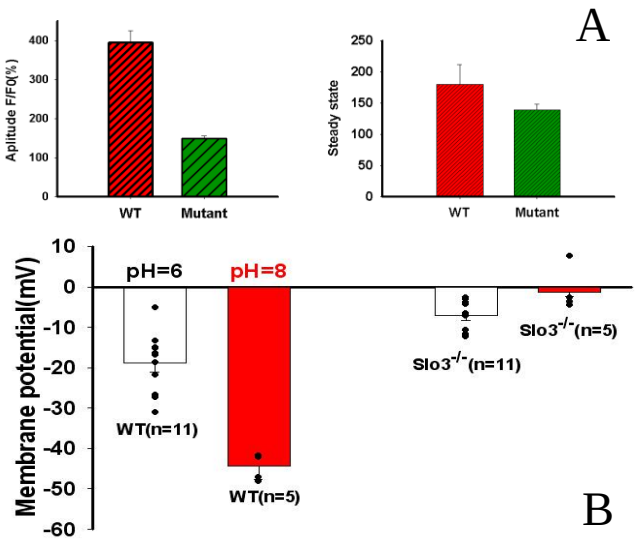

Figure 5: (A) Mean amplitude of NH_4Cl 10mM induced Ca^{2+} signals in Wild-type and $Slo3^{-/-}$ mutant mice (n=4). (B) is the steady state indced by NH_4Cl 10mM washout the relative inhibition of the Ca^{2+} signal amplitudes by QD 10 µM and Clofilium 50 µM in the presence of 10 mM NH_4Cl at PH 7.4 in both wild-type and $Slo3^{-/-}$ mutant mice (n=4) , data represented as mean ± St.error. (B). Membrane potentials of the wt and $Slo3^{-/-}$ sperms at pH_i= 6.0 and 8.0. Mean values of the membrane potentials measured with pippet saline at pH_i=6.0 and pH_i=8.0 (23) were -18.9±2.2 and -7.1±1.7 (n=11) at pH_i=6.0, and -44.3±1.4 and 1.39±2.3 (n=11) at pH_i=8.0 for the Wt and the $Slo3^{-/-}$ sperms as indicated, respectivel.

Simulation for the Ca^{2+} influx into sperms

Using the above functions, we can simulate the changes of Ca^{2+} in model sperm cells, while applying the inhibitors such as QD and Clofilium, and the **alkalize** NH_4Cl of CatSper and KSper channels (See the "Methods and Materials" and "Appendix"). Based on the transformation Eq. 11 of I_{Ca} and $[Ca^{2+}]_i$, we had the $I_{Ca}/I_{Ca0}=[Ca^{2+}]_i/[Ca^{2+}]_{i0}$ at steady state, indicating that the ratio I_{Ca}/I_{Ca0} can represent the steady-state relative intensity F/F_0 (%) in this study. Considering that all the chemicals were extracellularly applied onto sperms, we were not able to quantitatively estimate how much channels to be inhibited by 10 µM QD or 50 µM Clofilium. To match the data, in simulations, we thus assumed that 50 µM Clofilium blocked 18.5% $I_{Catsper}$ (Figure 4B) and 75% I_{Ksper} (22), and that 10 µM QD blocked 10% $I_{Catsper}$ (Figure 4A) and 55% I_{Ksper} (Figure 1A and 1B). To explore the role of Ksper channels, 50 µM Clofilium decreased the relative fluorescence intensities F/F_0 (%) about 38.0±5.9% (n=3) with an irreversible block for wt (Figure 7A1) and about 17 % (n=4) with a reversible block for $Slo3^{-/-}$ (Figure 7A2), consistent to the simulations (Figure 7B1-B2). This indicates that the Ksper (or Slo3) is able to enhance the intracellular $[Ca^{2+}]_i$ of sperms. Similarly, the 10 µM QD decreased the relative fluorescence intensities F/F_0 (%) about 18.8±5.1% (n=3) with an irreversible block for wt (Figure 7A3) and about 11% (n=4) with a reversible block for $Slo3^{-/-}$ (Figure 7A4), which is also consistent to our simulations on the ratio I_{Ca}/I_{Ca0} at steady-state levels (Figure 7B3-B4). This indicates again that the Ksper (or Slo3) play a critical role in regulating the intracellular $[Ca^{2+}]_i$ of sperms probably by enhancing the driving force of I_{Casper} channels.

To examine the pH effect of alkali agent NH_4Cl on both the Catsper and Ksper channels, we extracellularly applied the 10 mM NH_4Cl to the Wt and $Slo3^{-/-}$ sperms, respectively, and found that 10 mM NH_4Cl evoked a big Ca^{2+} surge in both the sperms (about 1.5-fold increase for Wt and 0.7-fold increase for $Slo3^{-/-}$) probably due to the big pH_i surge, the intracellular Ca^{2+}- release from Ca^{2+}-store and Ca^{2+} ion accumulation in sperms and then gradually went to the lower equilibrium levels, of which about 26% increase is for wt and 17% increase for $Slo3^{-/-}$.(Figure 7A5-A6). This indicates that alkaline environment can not only facilitate the Catsper channel to enhance the I_{Casper} current, but also the Ksper channel to increase the driving force of I_{Casper} channel, producing a significant influx into sperms. To match the data, in simulation, we thus assumed that the value of $[pH]_i$ would increase to 8.0 at the equilibruim state. Under this assumption, our simulations in both the cases displayed the corresponding increases at steady states (Figure 7B5-B6), consistent to the data (Figure 7A5-A6).

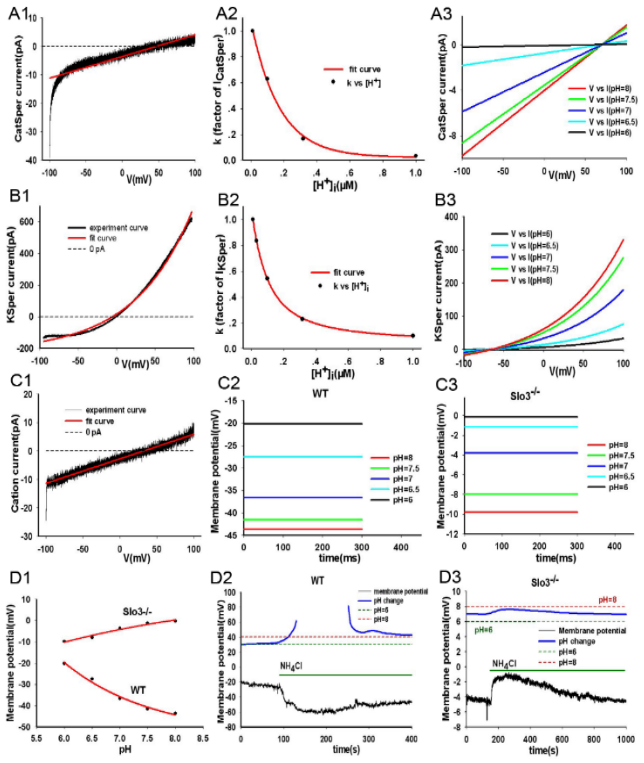

Figure 6. Constructing model channels (A) Left (A1), the CatSper current (black) at [pH]i=8.0, evoked by a ramp voltage protocol from -100 to +100 mV in the normal extracellular solution, was fitted to the Eq. 3 and Eq. 4 (See Methods and Materials). The fit line (red) showed a reversal potential of 47.1 mV. Middle (A2), the pH-dependence factor k(H^+) of ICatSper current (black circle) cited from the report by Kirichok et al (2006) was fitted to Eq. 5, where k(H^+)=1 at pH=8.0. The fit line is labeled in red. Right (A3), A set of simulated currents from Eq. 6 were plotted for ICatSper currents at pHi=6.0-8.0. (B) Left (B1), the KSper current (black) at [pH]i=7.4, evoked by a ramp voltage protocol from -100 to +100 mV in the symmetrical 160 K^+ solution, was fitted to the Eq. 7 and Eq. 8 (See Methods and Materials). The fit line (red) showed a reversal potential of -5.7 mV. Middle (B2), the pH-dependence factor k (H^+) of IKSper current (black circle), cited from the report by Navarro et al (2007), was fitted to Eq. 9, where k(H^+)=1 at pH=8.0. The fit line is labeled in red. Right (B3), A set of simulated currents from Eq. 10 were plotted for IKSper currents at pH_i = 6.0-8.0. (C) Left (C1), the cation current (black) at $[pH]_i$=8.0, evoked by a ramp voltage protocol from -100 to +100 mV in the normal extracellular solution, was fitted to the Eq. 12 and Eq. 13 (See Methods and Materials).The fit line (red) showed a reversal potential of 34 mV. Middle (C2), Simulations of membrane potentials was plotted for wt sperms at pH 6.0-8.0. Right (C3), Simulations of membrane potentials was plotted for Slo3$^{-/-}$ sperms at pH 6.0-8.0. (D) Left (D1). Two functions of Vm(pH)=-54.0903+1510.1986*exp(-0.6301*pH) and Vm(pH)= 13.2799-137.9215*exp(-0.2951*pH) were plotted for wt and Slo3$^{-/-}$ sperms, respectively, where Vm is the resting membrane potential.Simulations of membrane potentials was plotted for wt sperms at pH 6.0-8.0. Middle (D2), Membrane potential and simulation for pH change with the equation in (D1) was plotted for wild type sperms after adding NH4Cl. Right (D3), Membrane potential and simulation of pH change with the equation in (D1) was plotted for Slo3$^{-/-}$ sperms after adding NH4Cl.

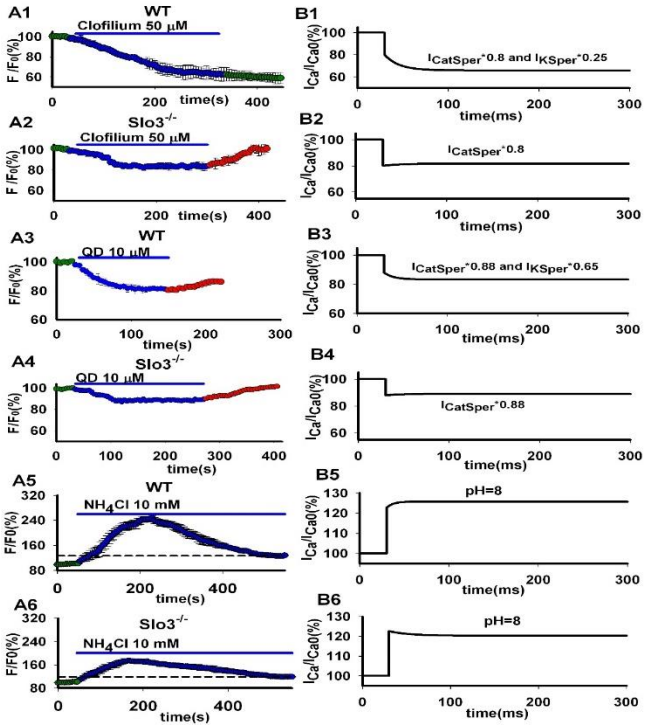

Figure 7. Simulations of I_{Ca}/I_{Ca0} currents of sperm heads in applying with QD., Clofilium and NH_4Cl. The mouse sperms were imaged with Flu4 –AM in the H.S. containing 2 mM $[Ca^{2+}]_i$ at pH_i= 7.4 as a control solution (green) as indicated. (A1-A3) the relative fluorescence intensities (F/F_0) (%) in WT mouse sperm (blue) as indicated has shown a 38.0± 5.9 % (n = 3) decrease at 50 µM clofilium (A1), and a 18.8± 5.06 % (n = 3) decrease at 10 µM QD (A3). (B1) The simulated line shows the I_{Ca}/I_{Ca0} in wt at 50 µM Clofilium, which was assumed to block 20% of CatSper currents and 75% of KSper currents. (B3) The simulated line has shown the I_{Ca}/ I_{Ca0} in the wt at 10 µM QD, which was assumed to block the only 12% of CatSper currents and 35% of KSper currents. (A2-A4) the relative fluorescence intensities (F/F_0) (%) in Slo3$^{-/-}$ sperm (blue) as indicated have shown a 17% ± 2.17 decrease (n=4) at 50 µM Clofilium (A2) and 11% ± 1.15 decrease (n

= 4) at 10 µM QD (A4), and then a complete recovery (red) after a washout with H.S at pH7.4 as indicated. (B2) The simulated line has the I_{Ca}/ I_{Ca0} in $Slo3^{-/-}$ at 50 µM Clofilium, which was assumed to block 20% of CatSper currents. (B4) The simulated line shows the I_{Ca}/ I_{Ca0} in $Slo3^{-/-}$ at 10 µM QD, which was assumed to block the only 12% of CatSper currents. (A5-A6) upon exposure to 10 mM NH_4Cl, the relative fluorescence intensities F/F_0(%) in the WT (A5) and $Slo3^{-/-}$ (A6) The sperms have shown a rapid increase to a plateau initially and then returns monotonically to the steady-state levels 126% for WT sperms (n = 5) (A5) and 117% for $Slo3^{-/-}$ sperms (n = 5) (A6), respectively, at 500 seconds. The dash lines in A5 and A6 denote the steady-state levels. (B5) The simulated line has the I_{Ca}/ I_{Ca0} in the wt at 10 mM NH_4Cl, which was assumed to increase the pH_i inside the sperms to 8.0 from 7.4. Under this assumption, our simulations show about 25.7**%** increase for WT. (B6) The simulated line shows the I_{Ca}/ I_{Ca0} in $Slo3^{-/-}$ at 10 mM NH4Cl, which was assumed to increase the pHi inside the sperms to 8.0 from 7.4. Under this assumption, our simulations show about 20.3**%** increase for $Slo3^{-/-}$.

Discussion

Recent work has demonstrated that the capacitation of sperms activated by membrane hyperpolarization resulting from Ksper activation under alkaline environment is critical for producing fertilization (2,22). However, it is difficult to rapidly judge the change of intracellular pH_i in sperm simply based on the change of fluorescence intensity as it is a more complex system, composed of a variety of Ca^{2+} sources such as Catsper channel, cation channel with a V_{rev}= +32 mV we found from the double KO mice and the intracellular Ca^{2+}-stores. Both the Catsper and Ksper channels in mouse spems are pH-dependent. Therefore, the intracellular pH_i is important parameter for understanding the mechanism affecting the ability of sperms to produce fertilization.The intracellular pH_i depends on the pKa (pK_a = 9.2 for NH_4Cl), which refers to the intracellular equilibrium $NH_4^+ \rightleftarrows NH_3+H^+$, and the ratio of $[NH_3]_i/[NH_4^+]_i$ (23) , that is, $pH_i=pK_a+\log([NH_3]_i/[NH_4^+]_i)$ Similalrly, for the extracellular pH_o can be written as the follows: $pH_o=pK_a+\log([NH_3]_o/[NH_4^+]_o)$. Since only the non-protonated form $[NH_3]_o$ diffuses through the plasma membrane, the equilibration between the external $[NH_3]_o$ and the internal $[NH_3]_i$ will be reached quickly. To calculate the pH_i , thus, it is sufficient to know the pH_o and the ratio between the internal and external amine concentrations reached at equilibrium. The internal pH_i can then be calculated using the following equation (24) $pH_i = pH_o - \log([NH_4^+]_i/[NH_4^+]_o)$. However, it is unkown about the $([NH_4^+]i$, which depends on Na-dependence of a sperm-specific Na^+/H^+ exchanger (sNHE) and a Na^+/HCO_3^- transport system in mouse sperms, powered by the energy stored in the inward Na^+ ion gradient, and the proton efflux through the proton channel H_{V1} (especially at $V_m > 0$ mV) in human sperms (12). In this study, we established a model based on the currents directly presenting in sperms instead of the kinetic models of corresponding channels, which not only allowed us to conquer a significant difficulty in kinetic modeling required for the HH-type model sperm, but also made us possible to adopt the suitable number n/n_0 for each channel to reach the savagery of sperms. During simulation, we found that the two-channel (Catsper and Ksper) model is impossible to match the data of pH_i and V_m unless adding a cation channel in the sperm model. This indicates that the cation channel must exist in mouse sperms. In this study, we ignored the Ca^{2+} contribution of the cation channel to sperms as the Ca^{2+} ions through cation channels were estimated about 10% of total ions.

We concluded from this study, the current model not only explains the capacitation mechanism induced by Ksper channels and introduces two functions of the pH_i and membrane potential Vm for quickly calculating the values of pH_i in wt and $Slo_3^{-/-}$ sperms according to the values of Vm measured by Current-Clamp experiments. Furthermore, we are able to infer the H^+ efflux derived from sNHE transport system or H_{V1} channel based on the pH_i changes in sperms. The method developed in this study may be useful for other physiological processes including nitrogen metabolism by the liver and acid-base transport by the kidney.

References

1. Navarro B, Kirichok Y, Clapham DE. KSper, a pH-sensitive K+ current that controls sperm membrane potential. Proc Natl Acad Sci U S A. 2007;104(18):7688-7692. doi:10.1073/pnas.0702018104.
2. Santi CM, Martínez-López P, de la Vega-Beltrán JL, Butler A, Alisio A, Darszon A, Salkoff L. The SLO3 sperm-specific potassium channel plays a vital role in male fertility. FEBS Lett. 2010;584(5):1041-1046. doi:10.1016/j.febslet.2010.02.005.
3. Schreiber M, Wei A, Yuan A, Gaut J, Saito M, Salkoff L. Slo3, a novel pH-sensitive K+ channel from mammalian spermatocytes. J Biol Chem. 1998;273(6):3509-3516. doi:10.1074/jbc.273.6.3509.
4. Austin C. Observations on the penetration of the sperm in the mammalian egg. Aust J Sci Res B. 1951;4(4):581-596. doi:10.1071/bi9510581.
5. Chang MC. Fertilizing capacity of spermatozoa deposited into the fallopian tubes. Nature. 1951;168(4277):697-698. doi:10.1038/168697b0.
6. Yanagimachi R. Fertility of mammalian spermatozoa: its development and relativity. Zygote. 1994;2(4):371-372. doi:10.1017/s0967199400002240.
7. Zeng Y, Oberdorf JA, Florman HM. pH regulation in mouse sperm: identification of Na(+)-, Cl(-)-, and HCO3(-)-dependent and arylaminobenzoate-dependent regulatory mechanisms and characterization of their roles in sperm capacitation. Dev Biol. 1996;173(2):510-520. doi:10.1006/dbio.1996.0044.
8. Demarco IA, Espinosa F, Edwards J, Sosnik J, De La Vega-Beltran JL, Hockensmith JW, Kopf GS, Darszon A, Visconti PE. Involvement of a Na+/HCO-3 cotransporter in mouse sperm capacitation. J Biol Chem. 2003;278(9):7001-7009. doi:10.1074/jbc.M206284200.

9. Handrow RR, First NL, Parrish JJ. Calcium requirement and increased association with bovine sperm during capacitation by heparin. J Exp Zool. 1989;252(2):174-182. doi:10.1002/jez.1402520209.
10. Florman HM, Jungnickel MK, Sutton KA. Regulating the acrosome reaction. Int J Dev Biol. 2008;52(5-6):503-510. doi:10.1387/ijdb.082696hf.
11. Zeng XH, Navarro B, Xia XM, Clapham DE, Lingle CJ. Simultaneous knockout of Slo3 and CatSper1 abolishes all alkalization- and voltage-activated current in mouse spermatozoa. J Gen Physiol. 2013;142(3):305-313. doi: 10.1085/jgp.201311011.
12. Chávez JC, Ferreira JJ, Butler A, De La Vega Beltrán JL, Treviño CL, Darszon A, Salkoff L, Santi CM. SLO3 K+ channels control calcium entry through CATSPER channels in sperm. J Biol Chem. 2014 Nov 14;289(46):32266-32275. doi: 10.1074/jbc.M114.607556.
13. Tang QY, Zhang Z, Xia XM, Lingle CJ. Block of mouse Slo1 and Slo3 K+ channels by CTX, IbTX, TEA, 4-AP and quinidine. Channels (Austin). 2010;4(1):22-41. doi:10.4161/chan.4.1.10481.
14. Wennemuth G, Westenbroek RE, Xu T, Hille B, Babcock DF. CaV2.2 and CaV2.3 (N- and R-type) Ca2+ channels in depolarization-evoked entry of Ca2+ into mouse sperm. J Biol Chem. 2000;275(28):21210-21217. doi:10.1074/jbc.M002068200.
15. Alghazal SM, Ding J, Hou P. Cytotoxic effect of Quinidine on testicular tissues, sperm parameters and Ca2+ level in mice sperms; as an option of male contraception. Advances Life Sci Technol. 2015;30:70-76. https://www.iiste.org/Journals/index.php/ALST/article/view/21127.
16. Hayashi H, Miyata H. Fluorescence imaging of intracellular Ca2+. J Pharmacol Toxicol Methods. 1994;31(1):1-10. doi:10.1016/1056-8719(94)90023-x.
17. Darszon A, Labarca P, Nishigaki T, Espinosa F. Ion channels in sperm physiology. Physiol Rev. 1999;79(2):481-510. doi:10.1152/physrev.1999.79.2.481.
18. Sun L, Xiong Y, Zeng X, Wu Y, Pan N, Lingle CJ, Qu A, Ding J. Differential regulation of action potentials by inactivating and noninactivating BK channels in rat adrenal chromaffin cells. Biophys J. 2009;97(7):1832-1842. doi:10.1016/j.bpj.2009.06.042.
19. Kirichok Y, Navarro B, Clapham DE. Whole-cell patch-clamp measurements of spermatozoa reveal an alkaline-activated Ca2+ channel. Nature. 2006;439(7077):737-740. doi:10.1038/nature04417.
20. Sun L, Xiong Y, Zeng X, Wu Y, Pan N, Lingle CJ, Qu A, Ding J. Differential regulation of action potentials by inactivating and noninactivating BK channels in rat adrenal chromaffin cells. Biophys J. 2009;97(7):1832-42. doi: 10.1016/j.bpj.2009.06.042.
21. Meuth SG, Bittner S, Meuth P, Simon OJ, Budde T, Wiendl H. TWIK-related acid-sensitive K+ channel 1 (TASK1) and TASK3 critically influence T lymphocyte effector functions. J Biol Chem. 200823;283(21):14559-14570. doi: 10.1074/jbc.M800637200.
22. Zeng XH, Yang C, Kim ST, Lingle CJ, Xia XM. Deletion of the Slo3 gene abolishes alkalization-activated K+ current in mouse spermatozoa. Proc Natl Acad Sci U S A. 2011;108(14):5879-5884. doi:10.1073/pnas.1100240108.
23. Musa-Aziz R, Jiang L, Chen LM, Behar KL, Boron WF. Concentration-dependent effects on intracellular and surface pH of exposing Xenopus oocytes to solutions containing NH3/NH4(+). J Membr Biol. 2009;228(1):15-31. doi:10.1007/s00232-009-9155-7.
24. Hamamah S, Gatti JL. Role of the ionic environment and internal pH on sperm activity. Hum Reprod. 1998;13 Suppl 4:20-30. doi:10.1093/humrep/13.suppl_4.20.

دراسة دور تيار قناة البوتاسيوم للتحكم في تدفق ايونات الكالسيوم والاس الهيدروجيني داخل نطف الفئران من خلال السيطرة على جهد الغشاء

سهى محمود أحمد الغزال[1] و جيوبنك دنك[2]

[1]فرع الفسلجة والكيمياء الحياتية والأدوية، كلية الطب البيطري، جامعة الموصل، الموصل، العراق، [2]المختبر الرئيسي للفيزياء الحيوية الجزيئية بوزارة التعليم، كلية علوم الحياة والتكنولوجيا، جامعة خواجونغ للعلوم والتكنولوجيا، ووهان ٤٣٠٠٧٤، الصين

الخلاصة

كان الهدف من هذا العمل هو استكشاف تفاصيل قنوات الأيونات ، و دورها الفسيولوجي في الحيوانات المنوية في المستقبل.عبرت الحيوانات المنوية للفئران باعتمادها على الاس الهيدروجيني لتيار قناة البوتاسيوم والذي يعتقد انه يحفز فرط الاستقطاب لتعجيل تدفق ايونات الكالسيوم من خلال التنشيط القاعدي لقنوات الكالسيوم لبدئ مايسمى بتهيئة الحيوانات المنوية للاخصاب بواسطة كلوريد الامونيوم خلال رحلتها في القناة التناسلية الانثوية لغرض الاخصاب.ومع ذلك ، فإن آلية تنظيم قنوات البوتاسيوم والكالسيوم من خلال جهد الغشاء والاس الهيدروجيني لاتزال غير مؤكدة، بسبب تعقيدات حركية اثنين من القنوات يصعب التغلب عليها في هذه المرحلة. هنا نوضح الاختلاف في تركيز ايونات الكالسيوم داخل الخلية مابين نوع الفئران من النمط البري والمطفرة جينيا (تم اعاقة عمل قناة البوتاسيوم) من خلال تعريضها لمثبطات قناة البوتاسيوم، الكواندين والكلوفيليوم وكلوريد الامونيوم ، اشرت الى ان قنوات البوتاسيوم وشفرة المورث هيمنت على جهد الغشاء لنطف الفئران لزيادة ايونات الكالسيوم والاس الهيدروجيني داخل الخلية من خلال عملية تهيئة النطف لممارسة دور مهم في عملية الاخصاب. علاوة على ذلك فأن النموذج المصصم لعمل النطف بنيت بشكل مباشر مع تيارات البوتاسيوم والكالسيوم في النطف والتي اظهرت وظيفتين لجهد الغشاء والاس الهيدروجيني داخل الخلية ، مما سمح لنا بحساب الاس الهيدروجيني داخل الخلية بواسطة كلوريد الامونيوم ، بناءأ على جهد الغشاء المسجل من تجارب المشبك الحالي . خلال النمذجة ، وجدنا قناة موجبة مع تيار+٢٠ ملي فولت في نطف الفئران المطفرة وراثيا (لقنوات الكالسيوم والبوتاسيوم) ، وهي بالتحديد ضرورية للنموذج للمقدرة على مطابقة البيانات.من الواضح، ان العمل الحالي ضروري لاستكشاف تفاصيل عمل هذه القنوات والدور الفسلجي للنطف في المستقبل